P13A.19

PRELIMINARY ANALYSIS OF A SEVERE WINTER STORM IN CENTRAL OKLAHOMA USING DATA FROM THE CASA, DUAL-POLARIZATION, DOPPLER-RADAR NETWORK

Jana Lesak Houser
Howard Bluestein
School of Meteorology, University of Oklahoma (OU), Norman, Oklahoma

1. INTRODUCTION

During the two-day period between 29 and 30 November 2006, a strong winter storm affected much of the state of Oklahoma, bringing a variety of frozen precipitation to the region. This was the first winter storm sampled by a mesoscale network of radars developed by the National Science Foundation's recently assembled Engineering Research Center for the Collaborative Adaptive Sensing of the Atmosphere (CASA). Although the network was designed primarily to observe severe weather, this study exemplifies the radars' ability to be useful for sampling winter weather

The storm had three distinct phases in its precipitation structure and dynamic characteristics: 1) an initial convective stage, during which many cells were electrically active, followed by 2) a transitional period associated with surface cyclogenesis to the southeast and a deepening upper-level trough to the northwest, resulting in the development of stratiform precipitation with embedded convective bands, and 3) the final phase characterized by light stratiform precipitation associated with the passage of the upper-level low.

The structure of this paper is as follows: first a brief description of the CASA network is presented followed by a summary of the synoptic conditions and evolution during the event, and a description of the three storm phases. Then the preliminary research completed thus far is described, including a brief examination of the two-dimensional wind field kinematics during the three phases of the storm, and a correlation between properties of the convective cells with lightning data obtained from the Oklahoma Lightning Mesonet Array.

2. CASA NETWORK

The CASA IP1 radar network, located in southwestern Oklahoma is comprised of four small, low powered dual-polarized radars designed to sample the lowest levels of the atmosphere typically missed by traditional National Weather Service Weather Surveillance Radars: 1988 Doppler (WSR-88D). They were also designed to collect data adaptively by determining areas of the greatest interest and modifying scanning strategies to most effectively sample a specific feature(s) through a process called distributive collaborative adaptive sensing (DCAS) (Brotzge and Droegemeier 2005).

The radars are located in Chickasha, Cyril, Lawton and Rush Springs, OK and are located within 50 km of each other. The instruments operate with a peak power of 25 kW, a wavelength of 3 cm, and a beamwidth of 2°. For this event, only the Rush Springs and Cyril radars were fully operational and collecting data for the duration of the storm.

3. SYNOPTIC CONDITIONS AND STORM PHASE DESCRIPTIONS

During the morning of 29 November 2006, a strong cold front associated with a surface low located in central Ontario passed through most of Oklahoma. The temperature gradient was generally on the order of 15° K over 100 km. At 500 hPa, a trough extended from North Dakota southwestward through eastern Arizona, lagging the surface cold front by nearly 1000 km. By 0000 30 Nov (all times in UTC), the cold front passed through all but the southeastern-most part of Oklahoma. The radiosonde data from Norman, OK (Fig. 1) at this time shows a

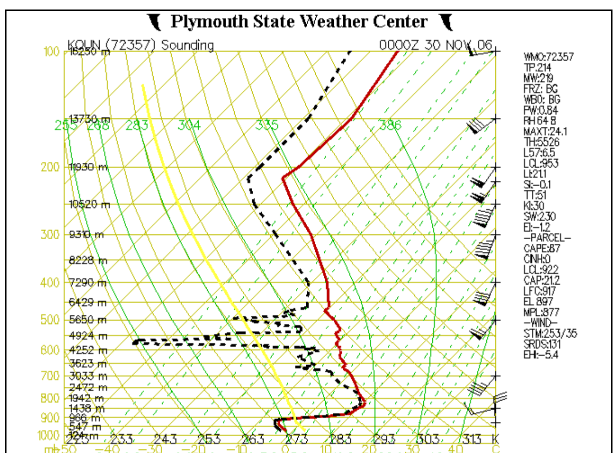

Fig. 1. 0000 UTC 30 Nov upper-air sounding from KOUN. Courtesy: Plymouth State archives.

shallow layer of subfreezing air below a very strong inversion at 800 hPa with a temperature of 10°C, above which there was a region of CAPE for elevated lift through 500 hPa.

The time between 1200 29 Nov and 0900 30 Nov corresponded with the first phase of precipitation in Oklahoma. During this period, a narrow convective line formed ahead of the cold front, followed by widespread convective cells that developed behind the front over the next several hours (Fig. 2a). The majority of precipitation during this time fell first as freezing rain then changed to sleet after about 0400.

By 1200 30 Nov, a secondary surface low developed in central Texas and a new wider swath of light to moderate precipitation, mainly falling as snow with some frozen precipitation mixing in occasionally, developed in response to

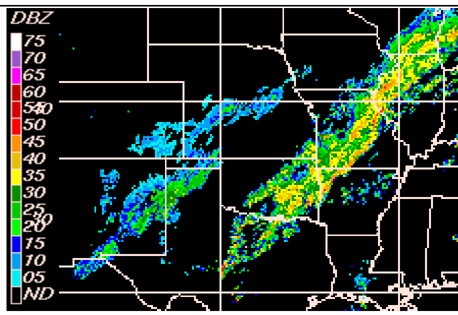

Fig 2a. National radar reflectivity mosaic from 0200 UTC 30 Nov depicting the convective phase.

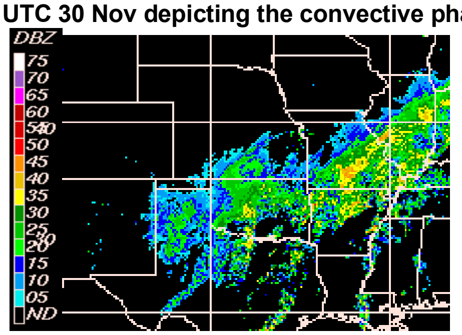

Fig. 2b. Reflectivity mosaic from 1400 UTC 30 Nov during the transitional phase.

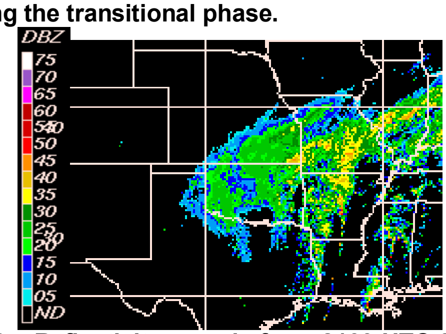

Fig. 2c. Reflectivity mosaic from 2100 UTC 30 Nov showing the upper level low passage phase. All images courtesy of NCDC.

the deepening upper level trough. The second period between 1200 and 2000 was a transitional period during which the convection associated with the surface front was replaced by more stratiform precipitation as the secondary surface low intensified to the southeast and the upper level trough deepened to the southwest (Fig. 2b). This phase was followed by the third and final stage of the storm associated with the passage of the upper level low. Precipitation falling during this time was all snow and was due to “wraparound” precipitation from the “comma head” structure formed by the upper level low (Fig. 2c).

4. DATA AND PRELIMINARY RESULTS

The data used in this study were collected by the Cyril and Rush Springs CASA radars. The radars’ scanning strategies included two 360° azimuth scans, one at an elevation angle of 1°, the other at 3°. Five times were selected for analysis from the three phases of the storm: 0215, 0245, 1315, 2045 and 2115 30 November. These times were chosen somewhat arbitrarily to include times with the best dual-Doppler data coverage, and to examine the rates at which the kinematics evolved during the first and last phases. The final times were chosen because the Cyril radar failed and became non-operational at 2117.

Data were objectively analyzed using the National Center for Atmospheric Research’s (NCAR) REORDER (Oye and Case 1995) program and a dual-Doppler analysis was performed using NCAR’s Cedric software (NCAR) to retrieve the horizontal wind components. Unfortunately, because data from higher elevations were unavailable, it was impossible to retrieve the vertical wind component accurately.

4.1 Rolls

Microscale boundary layer rolls were observed by both CASA radars in the velocity data during the 0215 and 0245 scans. Similar features also appeared in the WSR-88D KTLX and KFDR data at 0245, but did not exist at the earlier time (Fig. 3). The rolls appeared near the radar, at both elevation angles in the CASA data, and at 0.5° and 1.5° in the WSR-88D data. They were about 1 km in width and extended nearly 25 km horizontally from the radar corresponding to a vertical extent of approximately 700 m.

Although these rolls are interesting, their kinematic structure was irresolvable in the dual-Doppler analysis because their scale was too small. No explanation of forcing mechanisms for the rolls is offered here; however this will be investigated in future work. The main reason for examining the rolls is to provide a comparison of the features as observed by the WSR-88D and CASA instruments and to support the need for higher resolution instruments such as the CASA radars. At the location of the Rush Springs (RSP) radar, neither KTLX nor KFDR are able to resolve the roll features (Fig. 3c). At the lowest elevation angle, the KTLX beam is about 740 m above the ground. Although it is possible that the WSR-88D's cannot observe the rolls collocated with RSP because the beam overshoots the feature, it is more likely that the rolls cannot be resolved because the spatial resolution at this distance is coarse.

Fig. 3 shows the contrast between the rolls observed by RSP (Fig. 3a) and KTLX (Fig. 3b). Those sampled by the CASA radar have much higher resolution, better structure and were observed earlier. The rolls are visible in the KTLX data at a later time but are much less definitive. The KTLX image centered on RSP (Fig. 3c) does not indicate the presence of rolls. It does depict convergent and divergent features in the vicinity of RSP, but these are likely not associated with the rolls as they are not oriented properly. More likely they are a result of the rapidly backing wind field with height, as surface winds were northerly and those at 800 hPa were southwesterly.

4.2 Convective Phase Analysis

Dual-Doppler analyses were performed to examine the kinematics of the horizontal wind field every 100 m between the surface and 2 km in elevation. The analyses from the convective phase (0215 and 0245) suggest the wind field tended to be perturbed in the vicinity of higher reflectivity cores away from the baseline (Fig. 4a). This perturbation would indicate that potentially significant vertical velocities existed.

The data from the Oklahoma Lightning Mapping Array support this by showing prolific lightning activity associated with these the perturbed cores (Fig. 4b). Interestingly, some of the higher reflectivity cores did not appear to perturb the wind field at lower levels and these are associated with less frequent lightning. The convection during this period was likely due to a shallow layer of elevated convective available potential energy (CAPE) which existed above

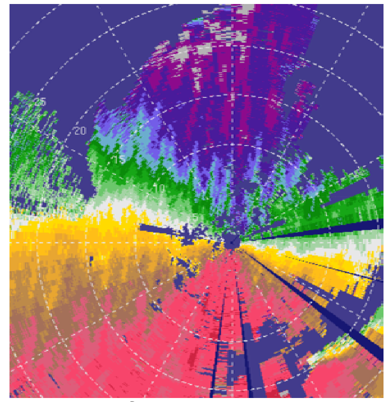

Fig. 3a. Velocity field depicting boundary layer rolls observed by RSP at 0215 30 Nov.

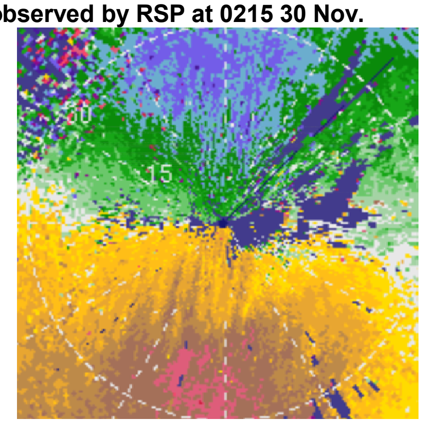

Fig. 3b. Velocity field depicting boundary layer rolls observed by KTLX at 0245 30 Nov.

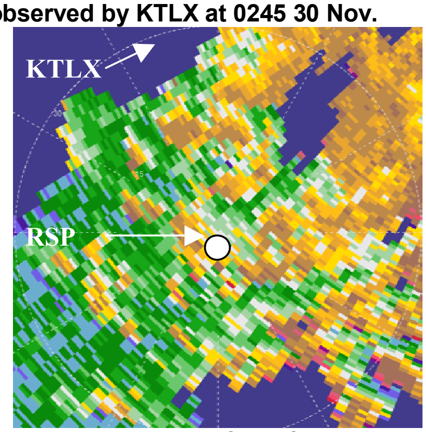

Fig. 3c. KTLX velocity field from 0215 30 Nov centered on RSP in the vicinity of the rolls. Spatial and velocity scales between RSP and KTLX are equivalent.

the inversion according to the 0000 30 Nov KOUN sounding (Fig. 1).

4.3 Transitional Phase Analysis

The 1315 scan taken during the transition time shows localized snow bands in the reflectivity field. These are hypothesized to be the result of conditional symmetric instability as no elevated CAPE existed in the 12Z KOUN upper air sounding and no evidence could be found of gravity wave passage in the Purcell profiler data. However, this has yet to be substantiated through a momentum and θ surface slope comparison. Dual-Doppler analyses from this time show winds primarily out of the north-northeast with some deviation around the banded features (Fig. 5a).

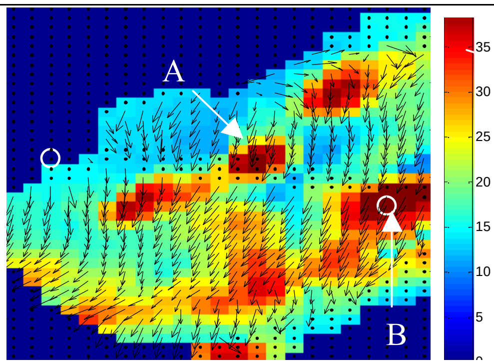

Fig. 4a. Interpolated reflectivity and dual-Doppler analyzed horizontal wind vectors for 500 m above ground from 0215 30 November. The Cyril and Rush Springs sites are depicted by the two white circles with RSP on the right. (Reflectivity and velocity vectors scaled for figure)

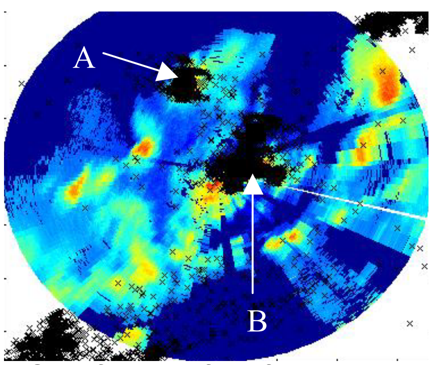

Fig. 4b. RSP reflectivity field for 0215 with lightning strike locations denoted by black x's. Lightning strikes are plotted for the time period between 0215 and 0217. Note, Fig 3a represents the left half of the images in Figs. 2b and 2c as beyond this, data were outside the dual-Doppler lobe.

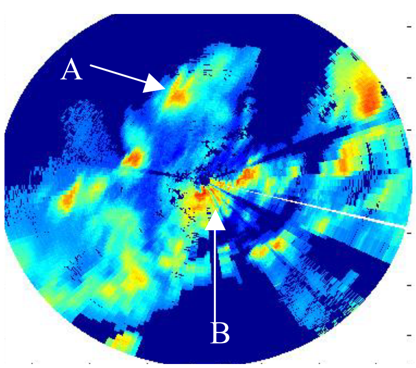

Fig. 4c. RSP reflectivity field for 0215 without lightning strikes.

4.4 "Wraparound" Phase Analysis

With the passage of the upper level low, the wind field exhibited constant northwesterly flow through 1.5 km, with little evolution between 2045 and 2115. Perturbations in the wind field for these times are small, occurred near the vicinity of the baseline and are likely spurious.

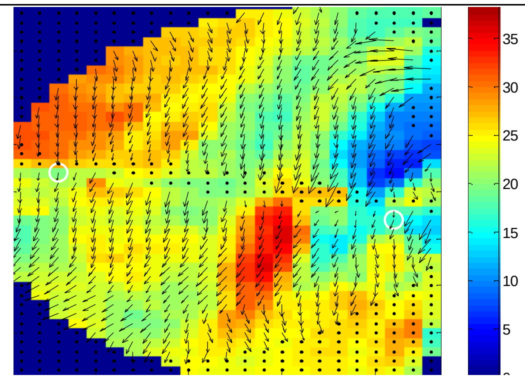

Fig. 5a. Interpolated reflectivity and dual-Doppler analyzed horizontal wind vectors for 500 m above ground from 1315 30 Nov.

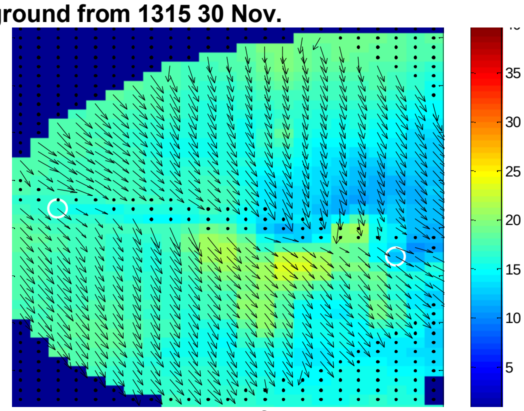

Fig. 5c. Interpolated reflectivity and dual-Doppler analyzed horizontal wind vectors for 500 m above ground from 2045 30 Nov.

4.5 Comparison between phases

From the dual-Doppler analyses of the horizontal wind field, velocity perturbation fields were generated by subtracting the analyzed wind vectors by the mean vector of the total field. Fig. 6 shows a comparison of the velocity perturbation fields for each phase. From the figure it can be seen that the perturbations are significantly greater for the convective phase than the other two, suggesting greater turbulent motion during this time. This period was also

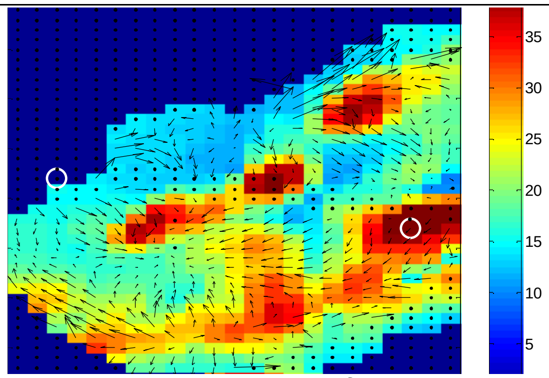

Fig. 6a. Velocity perturbations for 0215 30 Nov

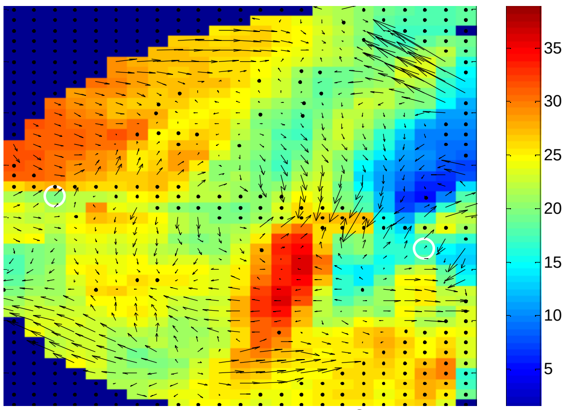

Fig. 6b. Velocity perturbations for 1315 30 Nov

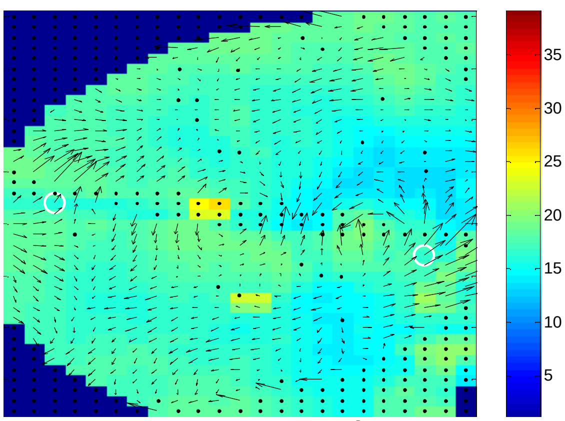

Fig. 6c. Velocity perturbations for 2115 30 Nov

characterized by greater temporal evolution of the wind field. The transition period still displayed significant deviations from the mean wind; however they are spatially more uniform. The final period shows comparatively less perturbations and those that are the most visible occur near the baseline and are therefore likely spurious.

5. CONCLUSIONS AND FUTURE WORK:

A winter-storm event that occurred from 29 to 30 Nov bringing freezing rain, sleet, and snow to much of Oklahoma, was sampled by the CASA radar network. These data were used to examine properties of the kinematics and dynamics associated with three distinct stages of the event: a convective, a transitional, and an upper-level low passage phase. Boundary layer rolls appeared in the CASA radar data that could not be seen with as much detail by the WSR 88-D radars nearby due primarily to poorer spatial resolution.

Dual-Doppler analyses revealed that the wind field during the convective period showed velocity perturbations in the vicinity of the updraft cores associated with electrical activity. During the transitional phase, snow bands were observed in the reflectivity field and were associated with small perturbations in the velocity field. As the upper level low passed, precipitation was light but constant and the wind field showed little perturbation from the overall environmental northwesterly flow.

In the future, the forcing mechanisms for the boundary layer rolls as well as those for the snow bands during the transitional phase will be examined. The dual-polarimetric variables will be compared with the KOUN data collected from the same time to examine the differences in data quality and to ensure the accuracy of the CASA radars' dual-pol measurements. Additionally, hydrometeor types and distributions will be determined from the CASA data and will be compared with lightning strike locations to examine the relationship between hydrometeor characteristics and cold-season lightning.

6. ACKNOWLEDGMENTS

The authors thank the National Science Foundation for providing support for this project through grant number EEC-0313747. Additionally, thank you to Jerry Brotzge for providing the CASA data; Nicole Lund for providing the lightning data; Yanting Wang and Brenda Dolan for helping with data translation; Curtis Alexander for providing technical support and code; Jeff Snyder and Robin Tanamachi for helping with graphical display; Jim Marquis, Paul Markowski and Yvette Richardson for helping to trouble-shoot and any other OU students or faculty that have contributed to this project.

7. REFERENCES

Brotzge, J. and K. Droegemeier, 2005: “Collaborative adaptive sensing of the atmosphere (CASA): A new radar system for improving analysis and forecasting of surface weather conditions.” Online.

NCAR, 1993: “Custom editing and display of reduced information in Cartesian space.” Manual.

Oye, D, and M. Case, 1995: “REORDER: A program for gridding radar data installation and use manual.” National Center for Atmospheric Research.